Chapter 6

Concentrated Photovoltaic (CPV): Hydrogen Design Methodology and Optimization

Muhammad Burhan,
Muhammad Wakil Shahzad and Kim Choon Ng

Additional information is available at the end of the chapter

http://dx.doi.org/10.5772/intechopen.78055

Abstract

To compete with the fossil fuel, there is a need for steady power supply from renewable energy systems. Solar energy, being highest potential energy source, is only available during diurnal period. Therefore, for steady power supply, an energy storage system is needed to be coupled with the primary solar energy system. For such application, hydrogen production is proved to provide long term and sustainable energy storage. However, firstly, there is a need to capture solar energy with higher efficiency for minimum energy storage and reduced system size. Concentrated photovoltaic (CPV) system, utilizing multi-junction solar cell (MJC), provides highest energy conversion efficiency among all photovoltaic systems. Despite, there is no model reported in the literature regarding its performance simulation and stand-alone operation optimization. None of the commercial software is capable of handling CPV performance simulation. In this chapter, a detailed performance model and an optimization strategy are proposed for stand-alone operation of CPV with hydrogen production as energy storage. A multi-objective optimization technique is developed using micro-GA for its techno-economic analysis. The performance model of MJC is developed based upon the cell characteristics of InGaP/InGaAs/Ge triple-junction solar cell. The system design is presented for uninterrupted power supply with minimum system cost.

Keywords: optimization, concentrated photovoltaic, genetic algorithm, hydrogen

1. Background

The global warming situations of 1.5°C rise in the average ambient temperature [1] are deemed inevitable due to the excessive emission of greenhouse gases such as carbon dioxide [2]. Today, renewable energy contributes only about 6.7% of the global energy demand [3]. The reason for the sluggish implementation of renewable energy sources can be attributed to their susceptibility to intermittency, low energy density and localized availability that make these energy sources mediocre as compared to the conventional fossil fuel-based sources. Among all renewable sources, solar energy has the highest potential [4] in meeting a significant portion of the total energy demand of future and for such an energy source to achieve sustainability, its energy quality and supply continuity are to be improved [5].

Current photovoltaic (PV) systems for electricity generation, available hitherto, comprises the stationary single junction silicon-junction-based solar cells such as mono-crystalline, poly-crystalline and thin films [6] with more than 98% share of photovoltaic market. Although such cells have a theoretical limit of 31% efficiency, the actual long-term electricity rating is merely less than 8% [7]. The advent of the third generation multijunction solar cells (MJCs), with the instantaneous cell-efficiency exceeding 46% [8] (but the quantum limit is 86%), has yet to receive widespread acceptance in form of concentrated photovoltaic (CPV) system in the current photovoltaic market. On the other hand, despite high-grade energy production as electricity, it is still intermittent and requires energy storage for steady power supply. Electrochemical storage in the form of battery does not make solar energy as a viable option to replace fossil fuels [9]. Electrolytic production of hydrogen by splitting water using solar electricity not only provides a portable green energy but also acts as high-density energy source, more than just energy storage [10]. The byproduct oxygen has many useful applications ranging from green disinfectant ozone to direct consumption in oxygen-based processes.

So far, in literature, all of the performance simulation models related to solar cells are based upon the single junction-based conventional flat plate PV systems. However, despite having the highest efficiency among all of the solar cells available hitherto [11], there is no performance models available in the literature that can simulate and predict the performance of multijunction solar cells in form of concentrated photovoltaic (CPV) systems. Therefore, as a sustainable energy source with highest solar electricity production efficiency, there is a need to develop a detailed performance optimization and simulation model for the standalone operation of CPV system, utilizing hydrogen as energy storage media. This chapter discusses the comprehensive model and optimization methodology for standalone and long-term operation of concentrated photovoltaic (CPV) with hydrogen production as energy storage and minimum cost. First, a detailed literature review of methodologies and commercial tools is presented. Second, an overall system model is presented, along with the system energy management and optimization methodology. Lastly, the optimized system design and corresponding performance parameters are presented and discussed.

2. Literature review

In order to compete with the conventional fossil fuels, the renewable energy resources must be able to provide uninterrupted power supply for any load demand, during whole day operation.

Such a requirement demands to operate them in standalone mode, without any external input. Therefore, such standalone operation requires the optimized size of each of the system component for uninterrupted power supply and for any load of the system, all the time with lowest overall system cost. Such standalone system design requires extensive system modeling with operational/optimization strategy/algorithm and economical information. In the design of any standalone system, there are three phases which have to be considered. In the first and most important phase, the main requirement is the selection of primary energy conversion system, which can have high efficiency and best performance with high power density. It also requires a detailed system modeling and control strategy of the system to be available to analyze the system performance under different conditions, for optimum design. If the main primary energy source is intermittent in nature, that is, renewable energy sources, the second phase is related to the selection of reliable, long-term and efficient energy storage system. The third and final step deals with the selection of the optimization algorithm which can handle multiple objective functions with less computational power and time to utilize the information received from the first two phases for the sizing of each component of the system.

Regarding the primary energy conversion system, as discussed earlier, concentrated photovoltaic system provides highly efficient solar energy conversion system among all of the photovoltaic units available hitherto. However, due to its intermittent nature and availability during diurnal period, an energy storage system is needed to be coupled for standalone operation and uninterrupted power supply by the system. As compared to the conventional electrochemical energy storage, that is, battery which is only suitable and economical for small-capacity system and short-term storage [12], electrolytic production of hydrogen provides a sustainable and long-term energy storage option, which can be easily converted into electricity when needed. It can also be transported from one place to another like conventional fuels. It can provide the most suitable long-term energy storage option for solar energy systems which a have life span of 20–25 years. Other energy storage methods like compressed air, pumped hydro, thermal storage and super capacitors do not provide either economical or long-term feasible options for such photovoltaic systems [13].

Regarding the third phase, related to optimization strategy and algorithm, there are many techniques available in the literature to do the job. However, the main requirement is to have an efficient and multiobjective solution in less possible time and computational power. The most common algorithm available in the literature is genetic algorithm (GA) which is based upon the concept of nature evolution [14] to optimize a set of design parameters for complex engineering systems. However, there are many new algorithms which have been claimed to be much more efficient than the conventional GA like particle swarm optimization (PSO). As both algorithms have different optimization and searching strategy [15], therefore, there is no benchmark where their performance can be compared. Overall, the PSO is claimed to be efficient as it takes less computational time [16]. Such a lack of performance is due to the large population size requirement of conventional GA. There are some variants of GA discussed in the literature, that is, NSGA-II and micro-genetic-algorithm (micro-GA) which are modified forms of conventional GA but eliminating its limitations for better performance [17]. Among all of the discussed optimization algorithms, micro-GA has been reported to have the best performance due to its small population size, as compared to NSGA-II and PSO [18]. It has shown better computational power with 8–12 times faster response and better Pareto front than NSGA-II [19]. Therefore, in this study, micro-GA is used as the optimization algorithm to optimize the overall size of standalone CPV-Hydrogen system.

Regarding system models and optimizations strategy, there are many studies in the literature which are related to standalone system size optimization and techno-economic evaluation. However, all of the studies related to photovoltaic system consider conventional flat plate single junction photovoltaic (PV) panels [20]. Even in hybrid renewable energy systems, utilizing wind turbine, battery, hydrogen, and so on, the main solar photovoltaic energy system is conventional PV [21]. All of the studies aim to increase the overall conversion efficiency of the primary energy system by utilizing its full potential, so that the overall size of the system can be reduced. On the other hand, due to many systems involved in hybridization, a complex control and energy management strategy is needed to operate the system. The concentrated photovoltaic (CPV) system provides the most efficient and simple photovoltaic technology for solar energy conversion, without any hybridization. However, there is no study in the literature that discusses the performance model and control strategy related to standalone operation of CPV. In addition, there are many commercial software related to simulation and optimization of renewable energy systems and their hybrids, for example, iHOGA, HYBRIDS2, INSEL, HOMER, TRNSYS + HYDROGEMS, SOMES, ARES, RAPSIM and SOLSIM [22]. But none of the software available hitherto has the capability to simulate and optimize the performance of concentrated photovoltaic (CPV) system. Therefore, the main objective of this chapter is to introduce and discusses the comprehensive model and optimization methodology for standalone and long-term operation of concentrated photovoltaic (CPV) with hydrogen production as energy storage.

3. Introduction to standalone CPV-hydrogen system

The simple schematic of concentrated photovoltaic (CPV) system with hydrogen as energy storage is shown in **Figure 1** for steady power supply and standalone operation. The concentrated photovoltaic (CPV) system, acting as primary energy supply unit, consists of multijunction solar cells (MJC)-based CPV modules, mounted onto two-axis solar trackers. As the solar concentrators require beam radiation for their operation, therefore, accurate two axis solar tracking is of prime importance for CPV operation. The arrangement of concentrating assembly of CPV system can be either a reflective type, that is, Cassegrain arrangement of reflectors or refractive type, that is, Fresnel lens. The developed performance model will be able to handle any type of concentrating assembly as it is based upon the final concentration ratio required by the MJC. For efficient CPV performance, maximum power point tracking (MPPT) device is attached to its output. The produced electricity after passing through MPPT device and DC/DC converter is supplied to the main DC line. The power consuming devices, such as solar trackers, take the power from main DC line for their operation.

The objective of targeted standalone CPV-hydrogen system is to provide an uninterrupted power supply to external consumer load, at any time and at level load level, by taking into account its own operational energy requirements. The consumer load is connected to the main

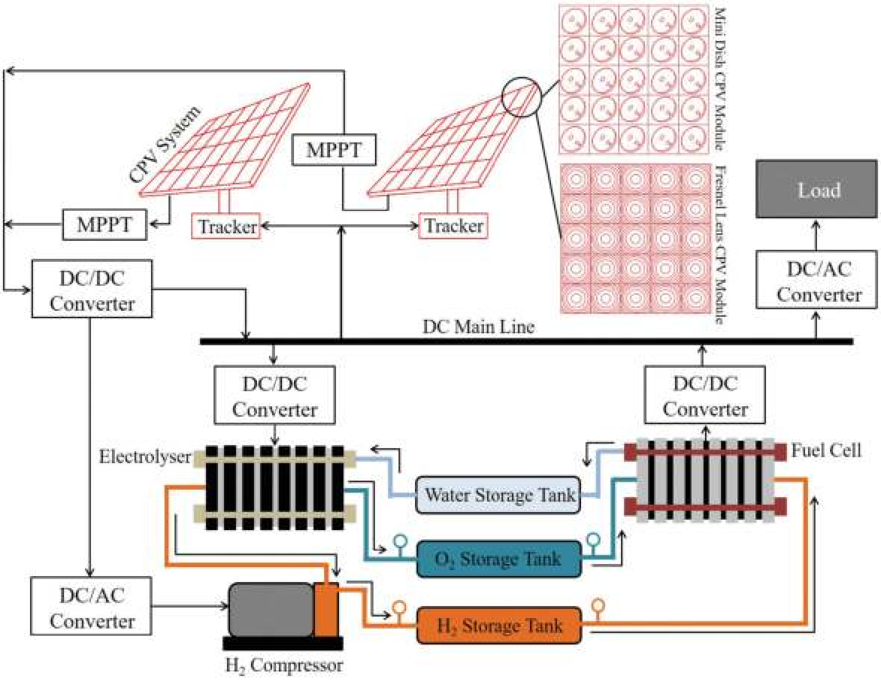

Figure 1. CPV-hydrogen system schematic for steady power supply and standalone operation [17].

DC line through DC/AC converter. The power supply to the consumer load is the first priority of the system, followed by the system operational needs. However, any excess power available is then supplied to the electrolyzer to produce hydrogen and oxygen by electrolytic splitting of water. The produced hydrogen is compressed and sent to tanks for storage and future use. However, the oxygen is stored at produced pressure as it can also be taken from environment in case of shortage. The power requirement of hydrogen compressor also comes from main DC line through DC/AC converter. In case of power deficit by the CPV system, the stored hydrogen is supplied to the fuel cell, with oxygen, to produce electricity and water. The produced electricity is then supplied to the main DC line through DC/DC converter. However, the produced water goes to storage tank, to be used as a loop in electrolyzer.

4. Performance model development for CPV-hydrogen system

In this section, detailed performance model of CPV-hydrogen system is discussed which is based upon the performance model of individual components which are linked together as a complete system through energy management strategy as shown in **Figure 2**. The main power input of the system is the solar energy in form of beam radiations or direct normal irradiance (DNI) as CPV cannot accept diffuse radiations. The weather data in the form of direct normal irradiance (DNI) are provided to the CPV performance model as input solar energy. The received solar energy is then used to calculate the concentration at the MJC area, according to the optical efficiency of the solar concentrators. By knowing the temperature characteristics of

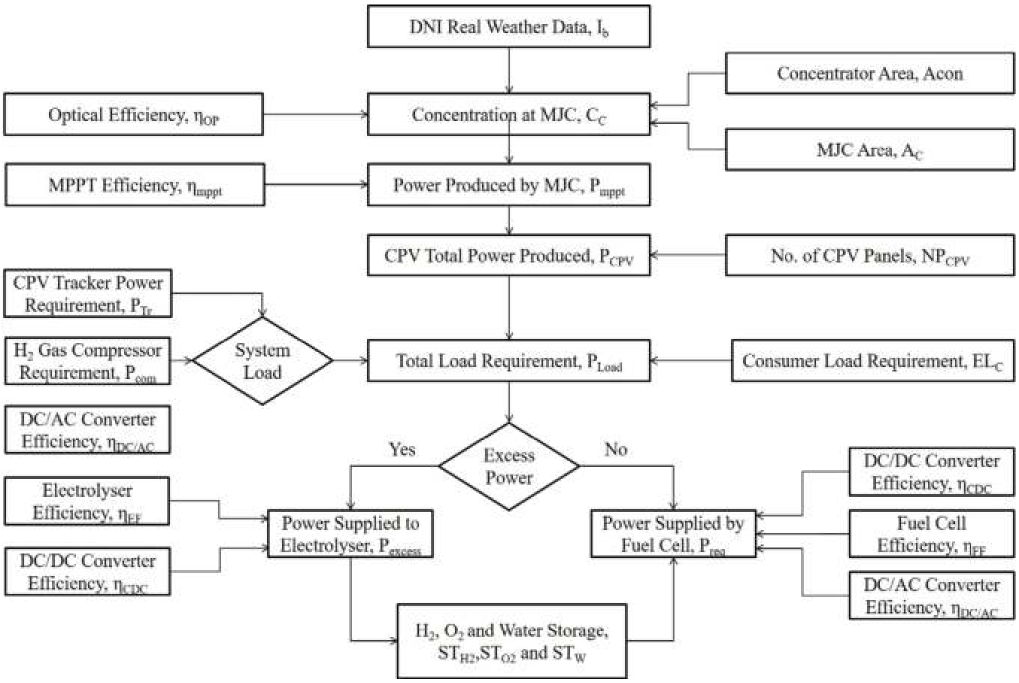

Figure 2. Energy management strategy for performance model of CPV-hydrogen system [17].

MJC and the total number of MJC units, the total power output from CPV can be calculated. Another input to the system performance model is the consumer electrical load requirements which is then combined with the system operational power requirements to calculated overall load of the system needed to be powered. The performance models for each individual components of the system are discussed later.

4.1. Concentrated photovoltaic system

The performance model of concentrated photovoltaic (CPV) system is based upon the single diode model, representing solar cell characteristic curves but considering concentration factor, is given by Eq. (1) [23].

$$P_C = I_C V_C = V_C \left[I_o \left\{ \exp\left(\frac{qV_C}{nkT_C} \right) - 1 \right\} - I_{SC} \right] \tag{1}$$

It must be noted that the values of all of the parameters appearing in the model of any component of the system are given in **Table 1**. For open circuit voltage, the diode saturation current factor "I_o" can be found by using V = V_{OC} and I = 0 in Eq. (1).

$$I_o = \frac{I_{SC}}{\left[\exp\left(\frac{qV_{OC}}{nkT_C} \right) - 1 \right]} \tag{2}$$

As the multijunction solar cells (MJC) can operate at higher concentrations, therefore, their performance characteristics are depending upon both temperature and concentration at cell area.

Parameter	Value	Parameter	Value
q (Coulomb) [24]	$1.6021765 \times 10^{-19}$	a1 [25]	0.995
k ($m^2kgs^{-2}\ K^{-1}$) [24]	$1.3806488 \times 10^{-23}$	a2 ($m^2\ A^{-1}$) [25]	−9.5788
n_C [24]	2	a3 ($m^2\ A^{-1}\ °C^{-1}$) [25]	−0.0555
η_{mppt} [26]	85%	a4 [25]	0
$\eta_{DC/AC}$ [27, 28]	90%	F (As mol^{-1}) [25]	96,485
η_{CDC} [29, 30]	95%	a5 ($m^4\ A^{-1}$) [25]	1502.7083
U_{rev} (V) [25]	1.229	a6 ($m^4\ A^{-1}\ °C^{-1}$) [25]	−70.8005
r_1 (Ωm^2) [25]	7.331×10^{-5}	a7 [25]	0
r_2 ($\Omega m^2\ °C^{-1}$) [25]	-1.107×10^{-7}	n [25]	2
S_1 (V) [25]	1.586×10^{-1}	U_o (mV) [25]	1065
S_2 ($V\ °C^{-1}$) [25]	1.378×10^{-3}	b (mV dec^{-1}) [25]	80
A_E (m^2) [25]	0.25	R (Ωcm^{-2}) [25]	0.438
S_3 ($V\ °C^{-2}$) [25]	-1.606×10^{-5}	M_{H2} (g/mol)	2.0159
t_1 ($m^2\ A^{-1}$) [25]	1.599×10^{-2}	CP_H (J/kg K)	14,304
t_2 ($m^2\ A^{-1}\ °C^{-1}$) [25]	−1.302	T_{com} (K)	306
t_3 ($m^2\ A^{-1}\ °C^{-2}$) [25]	4.213×10^2	$\eta_{DC/AC}$ (%)	90
r	1.4	η_{com} (%) [31]	70

Table 1. Information regarding constant factors appearing in CPV-hydrogen performance model.

The cell under consideration is a triple junction InGaP/InGaAs/Ge cell, for which the characteristics curves are shown in **Figure 3**. The short circuit current is proportional to the concentration ratio. However, open circuit voltage is following logarithmic variation against concentration ratio. In order to find out cell voltage and current, there is a need for "V_{OC}" and "I_{SC}" of cell to be known at that operating condition. If the trends of "V_{OC}" and "I_{SC}" are known at 25°C, then

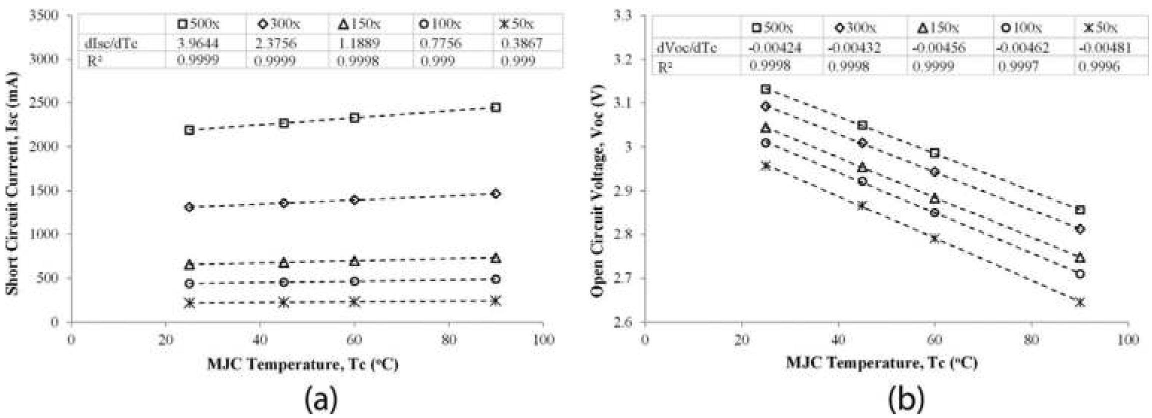

Figure 3. Variation in (a) short circuit current and (b) open circuit voltage of InGaP/InGaAs/Ge triple-junction solar cell with temperature and concentration [17].

their corresponding values at different temperature and concentration can be found using Eqs. (3) and (4).

$$V_{OC}(T_C, C_C) = [V_{OC}(at\ \ 25^oC)]_C + (T_C - 25)\left[\frac{dV_{OC}}{dT_C}\right]_C \tag{3}$$

$$I_{SC}(T_C, C_C) = [I_{SC}(at\ \ 25^oC)]_C + (T_C - 25)\left[\frac{dI_{SC}}{dT_C}\right]_C \tag{4}$$

Another required parameter is the cell temperature, which is assumed to be 40°C higher than the then ambient temperature, with 10°C temperature difference between cell surface and back plate temperature [32]. However, remaining temperature drop is between ambient and the heat sink/back plate. The concentration at cell area is given by Eq. (5).

$$C_C = I_b \times \frac{A_{con}}{A_C} \times \eta_{OP} \tag{5}$$

In order to model maximum power point tracking (MPPT) device, the derivative of cell power output equation can be equated to zero, as:

$$\frac{dP_C}{dV_C} = 0 \tag{6}$$

$$\frac{d}{dV_C}\left[V_C I_o\left\{\exp\left(\frac{qV_C}{nkT_C}\right) - 1\right\} - V_C I_{SC}\right] = 0 \tag{7}$$

After simplification, we can have the expression for power output of MJC as:

$$V_{mppt} = V_{OC} - \frac{nkT_C}{q}\ln\left[1 + \frac{qV_{mppt}}{nkT_C}\right] \tag{8}$$

$$\mathrm{I_{mppt}} = \mathrm{I_o}\left\{\exp\left(\frac{qV_{mppt}}{nkT_C}\right) - 1\right\} - I_{SC} \tag{9}$$

$$P_{mppt} = \eta_{mppt} \times I_{mppt} \times V_{mppt} \tag{10}$$

The simulated and experimental efficiencies of MJC are shown in **Figure 4**. By incorporating the efficiencies of voltage converters and the tracker power requirement, the net power output of CPV units is given by Eq. (11).

$$P_{CPV} = \eta_{DC/AC} \times \eta_{CDC} \times \eta_{Tr} \times P_{mppt} \times N_{CM} \times NP_{CPV} \tag{11}$$

For the current study, a CPV panel is assumed to be made of 25 MJCs, arranged into a 5 × 5 array. In addition, the power consumption of solar tracker is considered only during diurnal period, that is, from sunrise to sunset as calculated from solar geometry model [33].

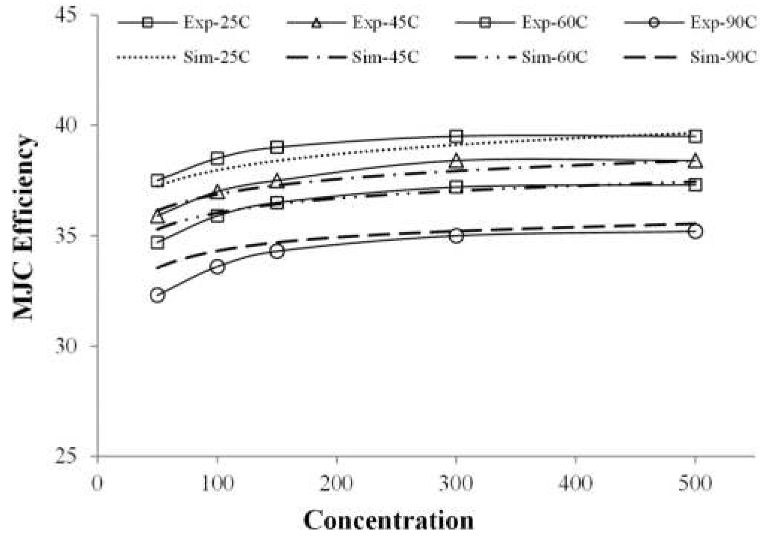

Figure 4. Comparison of experimentally measured and simulated efficiency of MJC at different concentrations and temperatures [19].

4.2. Electrolyzer

For the electrolyzer unit, the considered theoretical model is based upon the characteristics of an alkaline electrolyzer available in the literature [25]. The operating temperature of unit is assumed to be fixed at 80°C. The performance model for the operating voltage of single electrolyzer cell, under consideration, is given by Eq. (12).

$$U_E = U_{rev} + \frac{r_1 + r_2 T_E}{A_E} I_E + \left(S_1 + S_2 T_E + S_3 {T_E}^2\right).\log\left(\frac{t_1 + \frac{t_2}{T_E} + \frac{t_3}{{T_E}^2}}{A_E} I_E + 1\right) \tag{12}$$

It must be noted that the values of all required constant parameters are given in **Table 1**. The amount of hydrogen and oxygen production is based upon the amount of current passing through the electrolyzer and the Faraday efficiency, as given by Eqs. (13) and (14).

$$\dot{n}_{E,H2} = \eta_{EF} \frac{N_{EC} I_E}{nF} = 2\dot{n}_{E,O2} \tag{13}$$

$$\eta_{EF} = a_1.\exp\left(\frac{a_2 + a_3 T_E + a_4 {T_E}^2}{\frac{I_E}{A_E}} + \frac{a_5 + a_6 T_E + a_7 {T_E}^2}{\left(\frac{I_E}{A_E}\right)^2}\right) \tag{14}$$

In the design of the electrolyzer, the important parameter is the total number of cells needed. The number of electrolyzer cells depend upon the maximum amount of excess power that can be expected throughout the operational cycle of the system. By assuming the maximum rated current of 750 A and single cell voltage of 1.8 V [25], and the maximum MJC power output of 5 W, the required number of electrolyzer cells can be calculated as:

$$N_{EC} = \frac{(P_{MJC,\max} \times N_{CM} \times NP_{CPV}) - L_{\min}}{V_{EC,\max} \times I_{EC,\max}} \tag{15}$$

If the electrolyzer cells are assumed to be connected in series, then the current flow through the electrolyzer is given by Eq. (16). It must be noted that the excess power available must be calculated after fulfilling the total load requirements, that is, consumer load plus the system operational power requirement.

$$I_E = \frac{\eta_{CDC} \times P_{excess}}{N_{EC} \times U_E} \tag{16}$$

4.3. Fuel cell

For the current study, the proton exchange membrane (PEM) type of fuel cell is considered for which the performance characteristics are given in literature [25] and the performance model is given by Eq. (17).

$$U_F = U_o - b.\log\left(\frac{I_F}{A_F}\right) - R\left(\frac{I_F}{A_F}\right) \tag{17}$$

Like the electrolyzer, the gas consumption by fuel cell depends upon its total current flow, as per required power, which is given by Eq. (18). The amount of current flow through the fuel cell is given by Eq. (19), which is the same for each cell as they are connected in series. It must be noted that the fuel cell is assumed to be operated with a Faraday efficiency of 70% and the surface area for a single cell is taken as 300 cm^2.

$$\dot{n}_{F,H2} = \eta_{FF}\frac{N_{FC}I_F}{nF} = 2\dot{n}_{F,O2} \tag{18}$$

$$I_F = \frac{P_{req}}{\eta_{CDC} \times \eta_{DC/AC} \times N_{FC} \times U_F} \tag{19}$$

Like CPV and electrolyzer design, the fuel cell design is also based upon the maximum possible number of cells needed to meet the total load demand. As per the considered fuel cell characteristics [25], the maximum power per cell is 114.6 W. Therefore, for maximum load requirement of the customer, the total number of cells required in the design of a fuel cell is given by Eq. (19).

$$N_{FC} = \frac{L_{\max}}{\eta_{CDC} \times \eta_{DC/AC} \times P_{FC,\max}} \tag{20}$$

4.4. Hydrogen compressor

As mentioned earlier, the produced hydrogen is compressor by a mechanical compressor to be stored in the storage tank as the mechanical compression system provides a most compact and reliable storage solution. The performance model for mechanical compressor, for its power requirements, is based upon the thermodynamic equation depending upon the pressure ratio, that is, pressure at inlet and outlet of compressor, which is given by Eq. (21) [31].

$$P_{com} = \left(\dot{n}_{E,H2} \times \frac{M_{H2}}{1000}\right) \times CP_H \times \frac{T_{com}}{\eta_{DC/AC} \times \eta_{com}} \left\{ \left(\frac{P_{ta}}{P_E}\right)^{\left(\frac{r-1}{r}\right)} - 1 \right\} \tag{21}$$

It must be noted that the hydrogen produced by the electrolyzer goes to the compressor as they are connected in series. Therefore, the flow of hydrogen through compressor is the same as the rate of hydrogen production in electrolyzer. In addition, the compressor operating pressure is also assumed to be the same as the electrolyzer operating pressure as hydrogen directly goes to the compressor after production. The pressure at inlet of compressor is the same as the operating pressure of electrolyzer "P_E" and the pressure at the outlet of compressor is the same as the pressure inside storage tank "P_{ta}."

4.5. Hydrogen storage tank

In order to model the hydrogen storage tank, ideal gas equation is considered with compressibility factor "Z," as given by Eq. (22), to find out the tank pressure according to the stored amount of hydrogen.

$$P_{ta} = \frac{n_{ta} R T_{ta}}{V_{ta}} \times Z_H \tag{22}$$

$$Z_H = 3.5 \times 10^{-11} {n_H}^2 + 4.3 \times 10^{-5} n_H + 1 \tag{23}$$

A cylindrical tank of 3.34 m^3 capacity is considered and the Eq. (23) for compressibility factor for hydrogen storage tank is obtained from the actual gas pressure data obtained at 33°C from REFPROP (Reference Fluid Thermodynamic and Transport Properties), provided by NIST (National Institute of Standards and Technology) standard reference database Version 8.0 [34]. Eq. (22) for tank pressure, after putting the compressibility factor "Z," takes the final form as Eq. (24).

$$P_H = 2.666 \times 10^{-8} {n_H}^3 + 0.0032872 {n_H}^2 + 761.7476 n_H \tag{24}$$

5. Multiobjective optimization criteria

It has been mentioned that the main motivation of this study is to optimize the individual component of the CPV-Hydrogen system for uninterrupted power supply to consumer load, while meeting the system operational power requirements. However, for such system design problem, there can be many system size configurations that can fulfill the condition of steady power supply to the consumer. The main purpose of this optimization is to define a set of objective functions to look for system configuration which will not only provide uninterrupted power supply but at minimum cost and optimum system performance. Therefore, to achieve such a target, three objective functions are defined to be met as per proposed optimization strategy to find optimum system size configuration.

First, the main objective function defined is the power supply failure time (PSFT) which defines the number of seconds for which the system was unable to meet the total load requirements, that is, consumer load plus system operational power requirements. Such PSFT factor must be zero for any selected configurations, as given by Eq. (25). This objective function is of prime importance and has main priorities, before proceeding to the second objective function.

$$PSFT = \sum_{year} t_{PF} = 0 \tag{25}$$

In order to start the optimization simulation cycle, it is assumed that the gas storage tanks are filled with a certain amount of gases so that the optimization cycle can be started. Otherwise, in case of empty tanks, the simulation cycle will be stuck in achieving the first objective function if the input weather data value is poor at the start. However, at the end of the simulation cycle, such initial amounts of stored gases must be stored so that it can be assured that the system is self-sustaining and it was not operating because of the initial stored energy. Therefore, the second objective function for such a study is defined by Eq. (26).

$$L1 < ST_{H2(f)} - ST_{H2(i)} < L2 \tag{26}$$

where $ST_{H2(f)}$ and $ST_{H2(i)}$ define the state of the hydrogen storage tanks after and before the simulation cycle, respectively. On the other hand, L1 and L2 define the upper and lower limit of the difference between state of hydrogen tank before and after simulation cycle. The current simulation cycle is operated in a yearly manner. Therefore, the second objective function is computed at the end of each year. The value of L1 and L2 are selected as "−10" and "35," respectively, for the current study. The lower value L1 is kept minimum because it is desired that the system recovers to initial state at the end of the simulation cycle. However, the upper limit is kept a bit high so that system is well prepared for the simulation cycle and it can handle the load requirements with enough available storage, in case of poor weather conditions.

The last and the most important objective function is the overall system cost, including investment cost, operational cost and replacement cost. The overall system cost function is given by Eq. (27). The cost functions associated with individual components of the system are given by Eqs. (28)–(33). The system is operated for a lifetime of 20 years. Therefore, the cost parameters associated with each component of the system are given in **Table 2** [35]. In addition, the CRF (capital recovery factor) and the SPPW (single payment present worth) factor are also given by Eqs. (34) and (35). The interest rate considered in the current analysis is 6% [36].

$$C_{AT} = C_{CPV} + C_{EL} + C_{FC} + C_{STH2} + C_{STO2} + C_{com} \tag{27}$$

$$C_{CPV} = \left(NP_{CPV} \times N_{CM} \times P_{MJC,\max}\right) \times \left[CC_{CPV} + (OMC_{CPV} \times CRF)\right] \tag{28}$$

$$C_{EL} = (N_{EC} \times P_{EL,\max}) \times \left[CC_{EL} + (RC_{EL} \times SPPW) + (OMC_{EL} \times CRF)\right] \tag{29}$$

$$C_{FC} = (N_{FC} \times P_{FC,\max}) \times \left[CC_{FC} + (RC_{FC} \times SPPW) + (OMC_{FC} \times CRF)\right] \tag{30}$$

$$C_{STH2} = STM_{H2} \times [CC_{STH2} + (OMC_{STH2} \times CRF)] \tag{31}$$

$$C_{STO2} = STM_{O2} \times [CC_{STO2} + (OMC_{STO2} \times CRF)] \tag{32}$$

$$C_{com} = P_{com} \times [CC_{com} + (OMC_{com} \times CRF)] \tag{33}$$

$$CRF = \left[\frac{i \times (1+i)^L}{(1+i)^L - 1}\right] \tag{34}$$

$$SPPW = \frac{1}{(1+i)^y} \tag{35}$$

It must be noted that the cost associated with the voltage converters is assumed to be included in the cost of the primary component of the system. The solar trackers cost is included in the cost of the CPV system. However, cost for water storage is not considered due to its negligible effect on the overall system cost.

Component	CC	OMC	RC	Replacement
Hydrogen storage	666 $/kg	2% of CC	N.A.	N.A.
Oxygen storage	44.4 $/kg	2% of CC	N.A.	N.A.
Electrolyzer	3.774 $/W	2% of CC	0.777 $/W	10 years
Hydrogen compressor	3000 $/kW	20% of CC	N.A.	N.A.
Fuel cell	2.997 $/W	2% of CC	0.888 $/W	10 years
Concentrated photovoltaic (CPV)	2.62 $/W$_P$	2.125% of CC	N.A.	N.A.

Table 2. Costing parameters considered for techno-economic evaluation of CPV-hydrogen system [17].

6. System optimization algorithm and strategy with micro-GA

As mentioned earlier, the micro-genetic-algorithm (micro-GA) is considered as the main optimization algorithm to search for the optimum system configuration, as per defined objective functions. Based upon the defined performance model of CPV-Hydrogen system, the simulation and optimization program was developed in FORTRAN as per strategy shown in **Figure 5**. The program consists of two parts. The first part is associated with the performance simulation of CPV-Hydrogen system, based upon the developed model. The second part is associated with the system optimization, based upon the defined objective function, to find the optimum system size configuration using micro-GA. There are only two sizing parameters which are given as input to the program to be optimized, that is, the total number of CPV modules needed and the amount of initial hydrogen needed at the start of simulation and optimization cycle. However, the remaining parameters are calculated from these input parameters. The micro-GA is run with a population size of 5 and maximum 300 generations. The results of the study are presented in the next section.

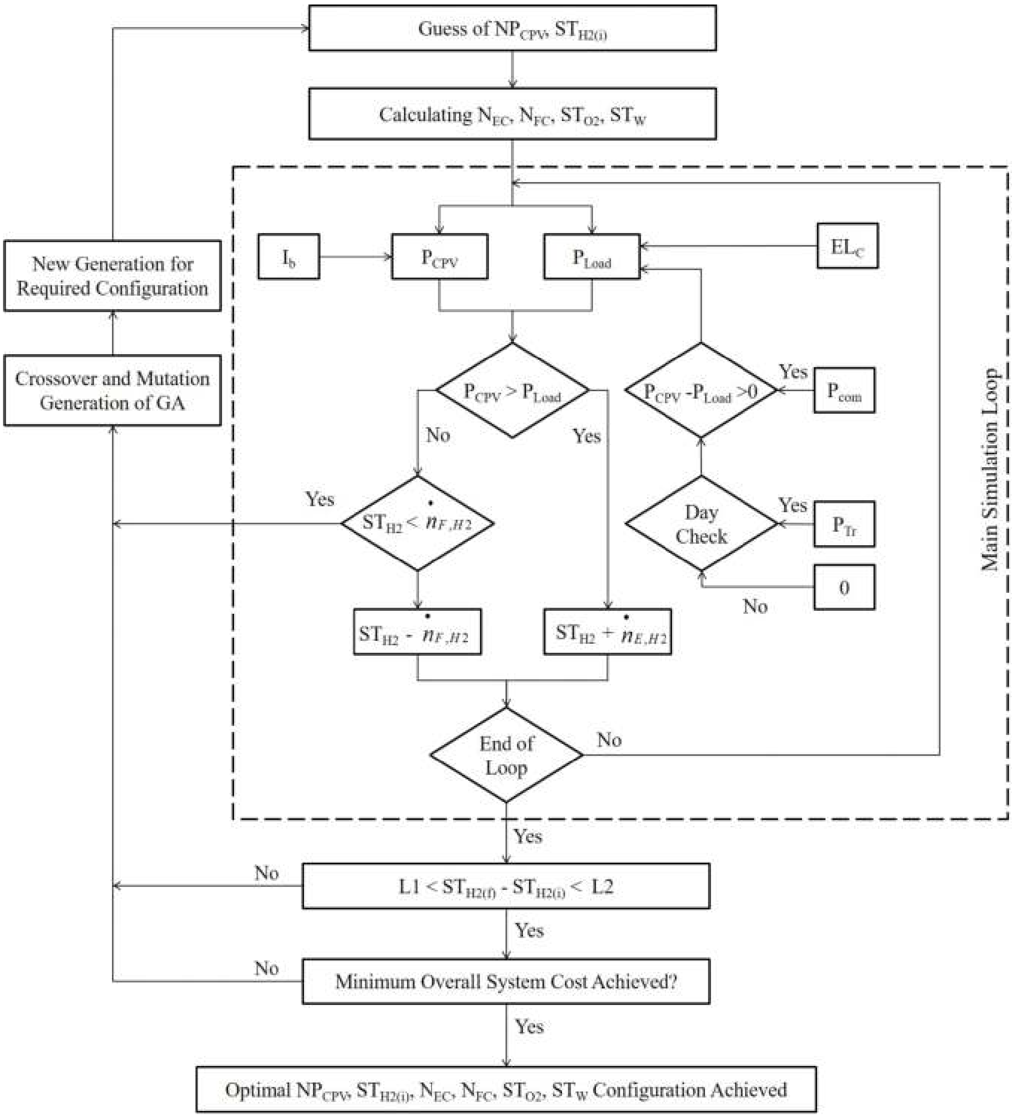

Figure 5. System size optimization strategy for standalone operation of CPV-hydrogen system [17].

7. Results and discussion

In order to simulate the system performance, the direct normal irradiance (DNI) data, obtained under tropical conditions of Singapore, at the rooftop of EA building of National University of Singapore, are shown in **Figure 6**. The DNI data were collected for a 1-year period from September 2014 to August 2015, at an interval of 1 s. To capture the DNI data, the pyrheliometer from Eppley Laboratory was mounted onto a two-axis solar tracker with tracking accuracy of 0.1°. **Figure 6** also shows the electrical load data, obtained from EMA (energy market authority) Singapore at an interval of 30 min. This acts as the input to the simulation cycle for

http://dx.doi.org/10.5772/intechopen.78055

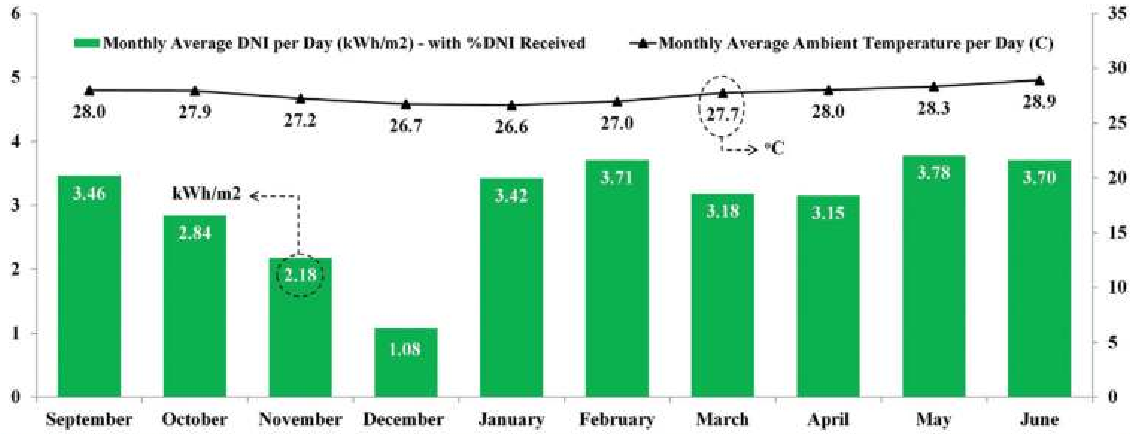

Electrical Load Profile

Time	12:00am	12:30am	01:00am	01:30am	02:00am	02:30am	03:00am	03:30am	04:00am	04:30am	05:00am	05:30am	06:00am	06:30am	07:00am	07:30am
Load(W)	5009.80	4774.90	4670.60	4586.50	4530.00	4472.30	4426.30	4413.70	4384.90	4385.90	4402.80	4467.50	4622.30	4827.30	5008.00	5171.50
Time	08:00am	08:30am	09:00am	09:30am	10:00am	10:30am	11:00am	11:30am	12:00pm	12:30pm	01:00pm	01:30pm	02:00pm	02:30pm	03:00pm	03:30pm
Load(W)	5366.90	5656.70	5864.10	6023.30	6089.60	6162.50	6221.10	6221.60	6206.10	6127.40	6131.70	6163.30	6209.00	6242.30	6224.20	6193.50
Time	04:00pm	04:30pm	05:00pm	05:30pm	06:00pm	06:30pm	07:00pm	07:30pm	08:00pm	08:30pm	09:00pm	09:30pm	10:00pm	10:30pm	11:00pm	11:30pm
Load(W)	6203.40	6203.80	6185.50	6152.90	6059.00	5921.20	5913.50	5942.40	5937.30	5904.60	5838.00	5781.70	5680.50	5493.50	5320.10	5169.70

Figure 6. DNI weather data and consumer electric load for Singapore [19].

consumer load demand. The actual load data were in megawatt units, which are scaled down to watts. The shown ambient temperature data were obtained from NEA (national environment agency) Singapore. The weather data shown in **Figure 6** act as the primary input for which the system performance is calculated and the optimum configuration of CPV-Hydrogen system is proposed.

As per the proposed system performance model, presented weather and load input data, energy management and optimization strategies and objective functions, the system optimization was performed by the developed program in FORTRAN using micro-GA. The optimization results are shown in **Figure 7**. From these results, it can be seen that the optimization calculations converge after 52 generations, with minimum overall system cost. It can also be seen that for all generations, the PSFT factor is zero and the difference between states of stored hydrogen, before and after the simulation cycle, is within the defined limits of L1 and L2. However, the stored hydrogen difference is closer to L1 limit, which shows that the system has successfully restored its state to initial conditions and it is ready for the next-year performance cycle. If the overall system cost is broken down, then the details are shown in **Figure 7**. It can be seen that the electrolyzer has the major cost proportion as 51%, followed by the CPV with 35%. In total, these two sub-systems account for 86% of the total system cost. It is important to mention here that the higher cost for electrolyzer is due to its replacement cost as the system has a lifetime period of 10 years and the overall CPV-Hydrogen system is targeted for a 20-year lifetime period.

In order to see the variations in the stored hydrogen energy against the operational period, the state of hydrogen and oxygen storage tanks is shown in **Figure 8**. It can be seen that the state of stored gases is decreasing during initial months of operation. This is because of the fact that for

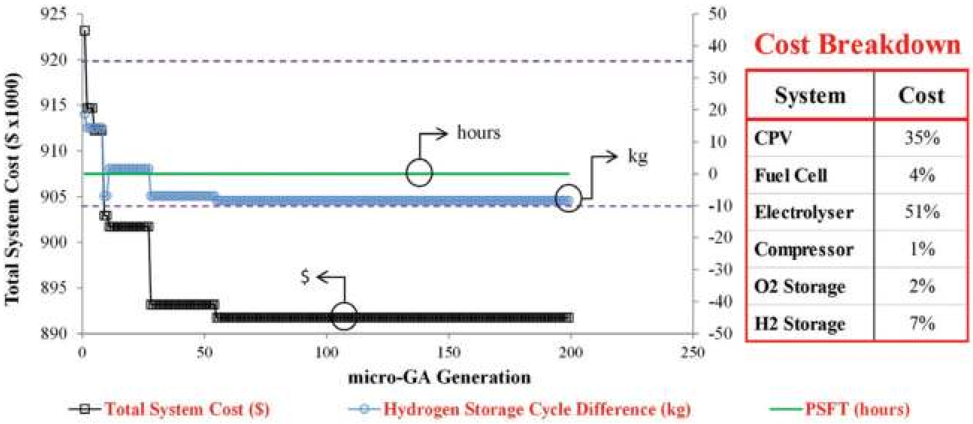

Figure 7. Optimization curve and cost breakdown of the system [19].

these months, the received DNI is also decreasing, which can be seen in **Figure 6**. These months represent the rainy season of Singapore and that is why the received DNI is lower for these months. The share of fuel cell, to meet the load demand during diurnal period, is also shown in **Figure 8**. It can be seen that the fuel cell share is also increasing for these months and for December, it hits about 60%. However, after this rainy season period, the state of energy storage tanks starts to recover and the received DNI as well as the fuel cell share also stabilize. But there is still about 25% fuel cell load share for each month. This is because of the tropical weather conditions as one cannot get clear sky for the whole day. However, the good thing is the stabilized weather conditions with less variations, which is good for the reliable operation of the designed system.

In order to further analyze the performance of CPV-Hydrogen system from its power production point of view, **Figure 9** shows the monthly average values of CPV electrical output and the Hydrogen output of CPV-Hydrogen system for the period of 1 year. The presented data are

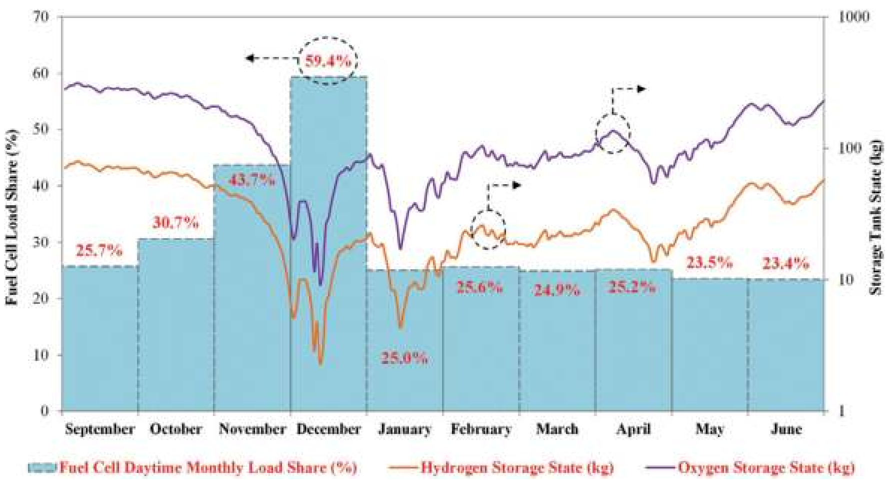

Figure 8. State of energy storage tanks and fuel cell share on monthly basis [19].

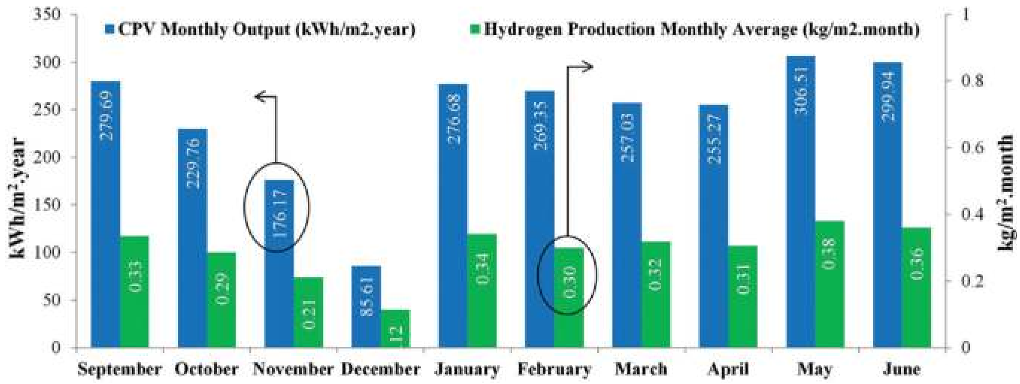

Figure 9. Summary of CPV-hydrogen system performance for electricity and hydrogen production [19].

normalized for per m^2 area. The trend of system output for both parameters is similar to the received monthly DNI, except for rainy season. The electrical output of the system dropped about three times in December than the usual operating month. That is why, a sharp decrease in the state of stored hydrogen was observed during this period. As the presented data are in per m^2 format, therefore, if the main objective of the system is to produce electricity or hydrogen, instead of standalone operation, then the system can be designed based upon the presented performance data.

Table 3 shows the overall summary of optimized CPV-Hydrogen system for standalone operation for defined objective functions and with minimum system cost. The interesting thing to be observed is that the power rating of electrolyzer is same as CPV. This is because of the fact that the design of electrolyzer is depending upon the maximum excess power available, which is proportional to the size of CPV. That is why a higher portion of cost was associated with the electrolyzer, even higher than the CPV. That was due to the replacement cost. It can also be seen that the power rating of CPV system is very large as compared to the consumer load. First, this is because of the fact that the system is designed to be operated in standalone mode while also meeting the system operational power needs, and at night, there is only stored hydrogen which can supply power to the load. Therefore, enough excess power is generated

Parameter description	Units	Value
No. of CPV modules		758
Rated power of CPV system	kW	94.75
Electrolyzer rated power	kW	91
No. of electrolyzer cells connected in series		67
Total hydrogen production	kg	622.22
Total oxygen production	kg	2469.23
Total water consumption	kg	2780.28
Fuel cell rated power	kW	7.33
No. of cells of fuel cell connected in series		64

Parameter description	Units	Value
Total hydrogen consumption	kg	630.55
Total oxygen consumption	kg	2502.28
Total water production	kg	2817.49
Hydrogen storage maximum	kg	81
Oxygen storage maximum	kg	319
Hydrogen storage maximum pressure	bar	200
No. of hydrogen storage cylinders	—	2
Maximum water storage tank	kg	358
Hydrogen compressor rated power	kW	1.13

Table 3. Summary of optimized CPV-hydrogen system design for standalone operation [17].

during the daytime to have enough storage for night operation. Second, as the weather input data were based upon tropical climate conditions, therefore, the system is oversized to have enough hydrogen generated to sustain during rainy period. This design summary is only for the mentioned location and the consumer load data. However, the main objective of proposing design methodology for standalone operation of CPV-Hydrogen system is achieved which can be easily implemented for any load requirement and weather conditions.

8. Summary of chapter

In order for the renewable energy sources to replace conventional fossil fuel-based energy sources, there is need for them to provide steady power supply for any load demand. Due to the intermittent nature of renewable energy sources, energy storage system is needed for steady power supply. Among all renewable energy sources, solar energy has the highest energy potential. But it is only available during diurnal period, with unsteady intensity. In order for such a system to compete with conventional fossil fuel-based system, there is a need for it to operate in standalone mode with sustainable and long-term energy storage system. For such standalone operations, it is very important to capture solar energy with high efficiency.

Photovoltaic system provides a most simple mean to convert sunlight into electricity and concentrated photovoltaic (CPV) technology provides the highest solar energy conversion efficiency among all photovoltaic systems. However, the entire photovoltaic market is dominated with conventional flat plate PV panels. In addition, the literature also focuses on the performance model and optimization strategy of conventional PV system, for its standalone operation. There is not even a single commercial software available which can handle CPV for the system performance analysis. Therefore, a detailed performance model and optimization strategy is proposed for standalone operation of CPV. For energy storage purpose, hydrogen is considered to provide a sustainable and long-term energy storage option than the conventional battery-based electrochemical storage.

http://dx.doi.org/10.5772/intechopen.78055

A detailed energy management technique, performance model and optimization strategy is proposed for standalone operation of CPV-Hydrogen system. The proposed model and strategy is successfully developed and implemented using micro-GA in FORTRAN programming. The overall system size is optimized for uninterrupted power supply to the consumer load with minimum cost. The proposed dynamic strategy is not based upon hourly performance of the system but it also restores the system to its initial state and prepares it for varying weather conditions. The system is not only designed to handle hourly weather variations but it also efficiently performs during seasonal weather variations. Such tech-economic optimization and analysis can be performed for any load demand and at any condition. Moreover, the proposed methodology can be integrated into commercial simulation tools so that they can become capable of handling CPV in their analysis.

Nomenclature

I_b	direct normal irradiance (DNI), (W/m^2)
A_{con}	area of solar concentrator (m^2)
A_C	solar cell area (m^2)
C_C	solar concentration at solar cell area (Suns)
I_C	solar cell current (A)
N_{CM}	number of solar cells in one panel
V_C	solar cell voltage (V)
NP_{CPV}	number of CPV panels
I_{SC}	solar cell short circuit current (A)
EL_C	electrical load demand of consumer (W)
V_{OC}	solar cell open circuit voltage (V)
ST_{H2}	state of hydrogen storage (kg)
T_C	solar cell temperature (°C)
ST_{O2}	state of oxygen storage (kg)
I_{mppt}	solar cell maximum power point current (A)
ST_W	state of water storage (kg)
V_{mppt}	solar cell maximum power point voltage (V)
STM_{H2}	maximum hydrogen storage capacity (kg)
P_C	solar cell power (W)

STM_{O2}	maximum oxygen storage capacity (kg)
P_{mppt}	solar cell maximum power point power (W)
η_{OP}	optical efficiency of concentrating assembly (%)
P_{CPV}	CPV power output (W)
η_{mppt}	Efficiency of Maximum Power Point Tracking Device (%)
P_{Load}	total load demand (W)
$\eta_{DC/AC}$	efficiency of DC to AC converter (%)
P_{excess}	excess available power from CPV (W)
η_{EF}	Faraday efficiency of electrolyzer (%)
P_{Tr}	solar tracker power requirement (W)
η_{CDC}	efficiency of DC to DC converter (%)
P_{com}	hydrogen compressor power (W)
η_{FF}	Faraday efficiency of fuel cell (%)
$P_{MJC,max}$	MJC maximum rated power (W)
η_{com}	efficiency of compressor (%)
$n^{\bullet}{}_{E,H2}$	hydrogen production flow rate from Electrolyzer (mol/s)
$n^{\bullet}{}_{F,H2}$	hydrogen consumption flow rate from fuel cell (mol/s)
$n^{\bullet}{}_{E,O2}$	oxygen production flow rate from electrolyzer (mol/s)
$n^{\bullet}{}_{F,O2}$	oxygen consumption flow rate from fuel cell (mol/s)
T_E	electrolyzer temperature (°C)
I_F	fuel cell current (mA)
I_E	electrolyzer current (A)
A_F	cell area of fuel cell (cm^2)
A_E	electrolyzer cell area (m^2)
U_F	cell voltage of fuel cell (mV)
U_E	electrolyzer cell voltage (V)
N_{FC}	number of cells of fuel cell
N_{EC}	number of cells of electrolyzer
$P_{FC,max}$	cell maximum power of fuel cell (W)
$V_{EC,max}$	electrolyzer cell maximum voltage (V)

http://dx.doi.org/10.5772/intechopen.78055

L_{max}	maximum electrical load requirement (W)
$I_{EC,max}$	electrolyzer cell maximum current (A)
P_{req}	electrical power deficiency not supplied by the CPV (W)
$P_{EL,max}$	electrolyzer cell maximum power (W)
U_o	reversible voltage of fuel cell (mV)
L_{min}	Minimum Electrical Load Requirement (W)
F	Faraday constant (A.s/mol)
U_{rev}	reversible voltage of electrolysis (V)
n	electrons requirement for water splitting
M_{H2}	molar mass of hydrogen (g/mol)
P_{ta}	instantaneous pressure of hydrogen tank (Pa)
CP_H	specific heat capacity of hydrogen (J/kg.K)
P_E	pressure of hydrogen production from electrolyzer (Pa)
T_{com}	hydrogen compressor temperature (K)
n_{ta}	instantaneous number of moles of hydrogen gas in storage tank (mol)
r	isentropic exponent of hydrogen
R	universal gas constant (J/mol.K)
Z_H	compressibility factor of hydrogen
T_{ta}	temperature of hydrogen storage tank (K)
V	volume of storage tank of hydrogen (m^3)
n_H	number of hydrogen stage tank
P_H	pressure of hydrogen storage tank (Pa)
t_{PF}	time for power failure (sec)
PSFT	power supply failure time factor (sec)
L2	maximum limit for cyclic hydrogen storage (kg)
L1	minimum limit for cyclic hydrogen storage (kg)
CC	capital cost ($)
C_{AT}	total annual system cost ($)
OMC	operation and maintenance cost ($)
C_{CPV}	CPV total cost ($)

RC	replacement cost ($)
C_{EL}	electrolyzer total cost ($)
CRF	capital recovery factor
C_{FC}	fuel cell total cost ($)
SPPW	single payment present worth
C_{STH2}	hydrogen storage total cost ($)
y	payment duration (years)
C_{STO2}	oxygen storage total cost ($)
i	compound interest rate (%)
C_{com}	hydrogen compressor total cost ($)
L	lifetime period of system (years)

Author details

Muhammad Burhan*, Muhammad Wakil Shahzad and Kim Choon Ng

*Address all correspondence to: muhammad.burhan@kaust.edu.sa

Biological and Environmental Science and Engineering Division, Water Desalination and Reuse Centre, King Abdullah University of Science and Technology, Saudi Arabia

References

[1] Trop P, Goricanec D. Comparisons between energy carriers' productions for exploiting renewable energy sources. Energy. 2016;**108**:155-161

[2] Ng KC, Burhan M, Shahzad MW, Ismail AB. A universal isotherm model to capture adsorption uptake and energy distribution of porous heterogeneous surface. Scientific Reports. 2017;**7**(1):10634

[3] Burhan M, Chua KJE, Ng KC. Electrical rating of concentrated photovoltaic (CPV) systems: Long-term performance analysis and comparison to conventional PV systems. International Journal of Technology. 2016;**7**(2):189-196. DOI: 10.14716/ijtech.v7i2.2983

[4] Burhan M, Oh SJ, Chua KJE, Ng KC. Double lens collimator solar feedback sensor and master slave configuration: Development of compact and low cost two axis solar tracking system for CPV applications. Solar Energy. 2016;**137**:352-363

[5] Burhan M, Shahzad MW, Choon NK. Hydrogen at the rooftop: Compact CPV-hydrogen system to convert sunlight to hydrogen. Applied Thermal Engineering. 2018;**132**:154-164

[6] Burhan M, Chua KJE, Ng KC. Simulation and development of a multi-leg homogeniser concentrating assembly for concentrated photovoltaic (CPV) system with electrical rating analysis. Energy Conversion and Management. 2016;**116**:58-71

[7] Burhan M, Shahzad MW, Ng KC. Long-term performance potential of concentrated photovoltaic (CPV) systems. Energy Conversion and Management. 2017;**148**:90-99

[8] Burhan M, Shahzad MW, Oh SJ, Ng KC. A pathway for sustainable conversion of sunlight to hydrogen using proposed compact CPV system. Energy Conversion and Management. 2018;**165**:102-112

[9] Burhan M, Oh SJ, Chua KJ, Ng KC. Solar to hydrogen: Compact and cost effective CPV field for rooftop operation and hydrogen production. Applied Energy. 2017;**194**:255-266

[10] Burhan M, Shahzad MW, Ng KC. Sustainable cooling with hybrid concentrated photovoltaic thermal (CPVT) system and hydrogen energy storage. International Journal of Computational Physics Series. 2018;**1**(2):40-51

[11] Muhammad B, Seung JO, Ng KC, Chun W. Experimental investigation of multijunction solar cell using two Axis solar tracker. Applied Mechanics and Materials. 2016;**819**:536-540. Trans Tech Publications

[12] Agbossou K, Kolhe M, Hamelin J, Bose TK. Performance of a stand-alone renewable energy system based on energy storage as hydrogen. IEEE Transactions on Energy Conversion. 2004;**19**(3):633-640

[13] Burhan M. Theoretical and experimental study of concentrated photovoltaic (CPV) system with hydrogen production as energy storage [Doctoral dissertation]; 2015

[14] Deb K. Genetic algorithm in search and optimization: the technique and applications. In: Proceedings of International Workshop on Soft Computing and Intelligent Systems, (ISI, Calcutta, India); 1998. pp. 58-87

[15] Bai Q. Analysis of particle swarm optimization algorithm. Computer and Information Science. 2010;**3**(1):180

[16] Shukla M, Dhaliwal BS. Review of Multi-objective Optimization using Genetic Algorithm and Particle Swarm Optimization. IP Multimedia Communications, A Special Issue from IJCA. pp. 72-74

[17] Burhan M, Chua KJE, Ng KC. Sunlight to hydrogen conversion: Design optimization and energy management of concentrated photovoltaic (CPV-hydrogen) system using micro genetic algorithm. Energy. 2016;**99**:115-128

[18] Choi S. Speedups for efficient genetic algorithms: Design optimization of low-boom supersonic jet using parallel GA and micro-GA with external memory. In: Genetic

Algorithms and Genetic Programming at Stanford. 2003. pp. 21-30. http://www.genetic-programming.org/sp2003/Choi.pdf

[19] Burhan M, Shahzad MW, Ng KC. Development of performance model and optimization strategy for standalone operation of CPV-hydrogen system utilizing multi-junction solar cell. International Journal of Hydrogen Energy. 2017;**42**(43):26789-26803

[20] Avril S, Arnaud G, Florentin A, Vinard M. Multi-objective optimization of batteries and hydrogen storage technologies for remote photovoltaic systems. Energy. 2010;**35**(12):5300-5308

[21] Dufo-López R, Bernal-Agustín JL, Contreras J. Optimization of control strategies for stand-alone renewable energy systems with hydrogen storage. Renewable Energy. 2007; **32**(7):1102-1126

[22] Bernal-Agustin JL, Dufo-Lopez R. Simulation and optimization of stand-alone hybrid renewable energy systems. Renewable and Sustainable Energy Reviews. 2009;**13**:2111-2118

[23] Nishioka K, Takamoto T, Agui T, Kaneiwa M, Uraoka Y, Fuyuki T. Annual output estimation of concentrator photovoltaic systems using high-efficiency InGaP/InGaAs/Ge triple-junction solar cells based on experimental solar cell's characteristics and field-test meteorological data. Solar Energy Materials & Solar Cells. 2006;**90**:57-67

[24] Cotal H, Sherif R. Temperature dependence of the IV parameters from triple junction GaInP/InGaAs/Ge concentrator solar cells. In: IEEE 4th World Conference on Photovoltaic Energy Conversion; Vol.1; 2006. pp. 845-848

[25] Ulleberg Ø. Stand-alone power systems for the future: optimal design, operation & control of solar-hydrogen energy systems [PhD Thesis]. Trondheim, Norway: Department of Thermal Energy and Hydropower, Norwegian University of Science and Technology; 1998

[26] Pan CT, Juan YL. A novel sensorless MPPT controller for a high-efficiency microscale wind power generation system. IEEE Transactions on Energy Conversion. 2010;**25**(1):207-216

[27] Chiu HJ, Lin LW. A high-efficiency soft-switched AC/DC converter with current-doubler synchronous rectification. IEEE Transactions on Industrial Electronics. 2005;**52**(3):709-718

[28] Ki SK, Lu DDC. Implementation of an efficient transformerless single-stage single-switch AC/DC converter. IEEE Transactions on Industrial Electronics. 2010;**57**(12):4095-4105

[29] Wang K, Lin CY, Zhu L, Qu D, Lee FC, Lai JS. Bi-directional DC to DC converters for fuel cell systems. In: Power Electronics in Transportation. IEEE; 1998. pp. 47-51. https://ieeexplore.ieee.org/abstract/document/731056/

[30] Nymand M, Andersen MA. High-efficiency isolated boost DC–DC converter for high-power low-voltage fuel-cell applications. IEEE Transactions on Industrial Electronics. 2010;**57**(2):505-514

[31] Li CH, Zhu XJ, Cao GY, Sui S, Hu MR. Dynamic modeling and sizing optimization of stand-alone photovoltaic power systems using hybrid energy storage technology. Renewable Energy. 2009;**34**(3):815-826

[32] Yu X, Gen M. Introduction to Evolutionary Algorithms. London: Springer Science & Business Media; 2010

[33] Oh SJ, Burhan M, Ng KC, Kim Y, Chun W. Development and performance analysis of a two-axis solar tracker for concentrated photovoltaics. International Journal of Energy Research. 2015;**39**(7):965-976

[34] REFPROP Reference Fluid Thermodynamic and Transport Properties. National Institute of Standards and Technology (NIST) Standard Reference Database 23, Version 8.0. http://www.nist.gov

[35] Simbeck D, Supply CEH. Cost Estimate for Hydrogen Pathways—Scoping Analysis. Mountain View, California: SFA Pacific, Inc.; 2002. NREL

[36] Rehman S, Al-Hadhrami LM. Study of a solar PV–diesel–battery hybrid power system for a remotely located population near Rafha, Saudi Arabia. Energy. 2010;**35**(12):4986-4995